INSTITUTE OF PHYSICS PUBLISHING JOURNAL OF PHYSICS B: ATOMIC, MOLECULAR AND OPTICAL PHYSICS

J. Phys. B: At. Mol. Opt. Phys. **38** (2005) S363–S371 doi:10.1088/0953-4075/38/2/027

Propagation of double Rydberg wave packets

F Robicheaux[1] **and R C Forrey**[2]

[1] Department of Physics, Auburn University, Auburn AL 36849, USA
[2] Pennsylvania State University, Berks-Lehigh Valley College, Reading PA 19610, USA

E-mail: robicfj@auburn.edu

Received 22 June 2004
Published 5 January 2005
Online at stacks.iop.org/JPhysB/38/S363

Abstract

Double Rydberg wave packets for He electronic states are propagated in time using fully quantum mechanical calculations. The wave packets are constructed so that the two electrons are simultaneously excited up to $n_{\mathrm{Ryd}} \sim 15$ states and coupled to total orbital angular momentum equal to zero and to total spin equal to zero. We attempt to construct a wave packet to isolate symmetric stretch motion. Classical and quantum ideas are used to interpret several features of the time-dependent wave function. We briefly discuss some of the interesting problems that can be addressed.

A recent area of research is the time development of electron wave packets in two or more spatial dimensions [1–14]. This interest has been sparked by the ability of experimentalists to initiate and measure the time-dependent behaviour of quantum systems *and* by the increase in computational power and numerical sophistication that allows calculations for complex systems. Another reason for this interest is that it is instructive to observe quantum systems in ways that are quite similar to analogous classical systems. In atomic physics, the motion of one electron wave packets has proved to be an interesting playground for enhancing our ideas about the flow of energy and probability through different degrees of freedom [9–14].

There have been a few steps in the next obvious direction in which two electrons participate in the wave packet motion in a nontrivial manner [1–8]. In the early studies, both electrons are excited above the ground state although at least one of the electrons has been restricted to a quite small distance, typically less than 5 Bohr radii. Thus, quantum effects completely dominate the behaviour of one of the electrons and it is not possible to establish a correspondence with classical dynamics. Very recently, Pisharody and Jones [8] have observed wave packet behaviour for two electrons when they can both be simultaneously at large distances. The results of this measurement were interpreted using classical trajectories and simplified quantum models. Although the simplified models reproduce the main features of the experiment, it is clearly time for a strong theoretical effort to perform fully quantum calculations of double Rydberg wave packets.

In this paper, we show how it is possible to extend the range of motion that can be theoretically investigated by performing accurate and fully quantum calculations where both

electrons are simultaneously ∼300 Bohr radii from the nucleus. The wave packets are for electrons simultaneously in $n_{\rm Ryd} \sim 15$ states; both electrons are in the semiclassical limit and some correspondence with classical motion may be observed. For all the calculations presented in this paper, the angular momentum and spin of the two electrons are coupled together so that both the total orbital angular momentum and the total spin are zero. This reduces the 6-degrees of freedom to 3; but this is the only restriction and we attempt to account for the remaining three dimensions as accurately as possible using an efficient basis set expansion. The wave packets discussed here are true He wave packets and are not wave packets for a simplified model. The main result presented here is the knowledge that double Rydberg wave packets can be generated and investigated with quite modest resources; all the calculations for this paper were performed on a personal computer. We discuss the various possible choices for the computational techniques and the physics that determines which techniques might be best. The other main result pertains to one of the simplest investigations into the dynamics of two electron states. This investigation confirms some of our expectations but also demonstrates that many aspects of the time-dependent wave function can be understood at a qualitative level.

The ability to obtain accurate time-dependent wavefunctions depends on how efficiently it can be represented and on the level of complexity of the wavefunction. Typically, the level of difficulty increases with the number of nodes in the wavefunction and with the number of spatial dimensions. There are two generic possibilities for representing the wavefunction: basis function techniques and a grid of spatial points. Basis functions can often represent the wavefunction with relatively few functions but sometimes the resulting representation of the Hamiltonian is dense; thus the number of Hamiltonian matrix elements scale with the square of the number of basis functions. A spatial grid of points usually gives a sparse representation of the Hamiltonian, but sometimes the number of points needed for an adequate description of the wavefunction is large.

Wintgen and co-workers [15–17] showed that a Sturmian basis set in perimetric coordinates gave an extremely efficient representation of highly excited resonance states of He. The perimetric coordinates are $q_{12} = r_1 + r_2 - r_{12}$, $q_1 = -r_1 + r_2 + r_{12}$ and $q_2 = r_1 - r_2 + r_{12}$. The basis functions are chosen to be

$$y_{n_{12},n_1,n_2} = \phi_{n_{12}}(2\beta q_{12})\left[\phi_{n_1}(\beta q_1)\phi_{n_2}(\beta q_2) + \phi_{n_1}(\beta q_2)\phi_{n_2}(\beta q_1)\right]\Big/\sqrt{1+\delta_{n_1,n_2}} \tag{1}$$

with $\phi_n(x) = L_n(x)\exp(-x/2)$ and where $L_n(x)$ are the usual Laguerre polynomials. When the electrons' spins are coupled to total spin 1, the + is replaced by −. The parameter β is a scale parameter which sets the size of the wavefunction. When trying to model the motion of two electrons both with principal quantum number $n_{\rm Ryd}$, a decent choice for β is $2/n_{\rm Ryd}$. The symmetry of the functions means that only $n_1 \leqslant n_2$ is needed in the basis set. Our basis set includes all functions with $\omega \equiv n_{12} + n_1 + n_2 \leqslant \omega_{\rm max}$. The number of basis functions is the nearest integer to $\omega_{\rm max}^3/12 + 5\omega_{\rm max}^2/8 + 17\omega_{\rm max}/12 + 7/8$.

A very nice property of this basis set is that the Hamiltonian and overlap matrices are extremely sparse in this representation. Another advantageous property is that a complex scaling of the coordinates may be employed; thus, in principle it is not necessary to include the electron continuum states since any outgoing flux is àbsorbed' in the complex plane. The resonance states have complex energies and their norm decreases exponentially with time. As discussed below, we could not take advantage of complex scaling in our time-dependent calculations.

For the time-dependent wavefunctions, we found that the sparseness of the Hamiltonian and overlap matrix contributed greatly to the ability to increase the size of the basis set and to increase the speed of the calculation. We were thus able to obtain converged results for both electrons in $n_{\rm Ryd} = 16$ states on a small PC with 250 Mb of RAM. The nondiagonal

overlap matrix does not have a negative effect on the calculations presented here since we used an implicit method to propagate the wavefunction as discussed below; however, the overlap matrix effectively eliminates the possibility of using a direct time propagation of the wavefunction since it is necessary to invert the overlap matrix at each time step.

The only unforeseen difficulty arose when we tried to use complex scaling to take care of the outgoing waves. There is more than enough energy for one of the electrons to escape the atom; these outgoing waves reflect from the edge of the basis set. Although complex scaling works perfectly well for time-independent calculations of resonance parameters, it works very poorly for this time-dependent problem. The reason is that unless $|\beta|$ is larger than ~ 1.7 there are always some eigenvalues of the time-independent problem that have *positive* imaginary parts which causes an exponential divergence of the wavefunction with time. Unfortunately, such a large value of $|\beta|$ completely destroys the usefulness of the basis set for describing Rydberg states. Thus, we could not use complex scaling and were forced to use a mask at the edge of the basis set. The mask was a diagonal function of $\omega = n_1 + n_2 + n_{12}$ instead of a diagonal function of the distances. All the results presented here were tested for their dependence on the range and strength of the masking function.

The wavefunction is expanded in a time-independent basis set. Letting N stand for the triple index n_{12}, n_1, n_2 we write

$$|\Psi(t)\rangle = \sum_N |y_N\rangle C_N(t) \tag{2}$$

with the differential equation for the C_N given by

$$\mathrm{i}\sum_N O_{N'N}\dot{C}_N(t) = \sum_N H_{N'N}C_N(t) \tag{3}$$

where $O_{N'N} = \langle y_{N'}|y_N\rangle$ and $H_{N'N} = \langle y_{N'}|H|y_N\rangle$. Integrating this equation from t to $t + \delta t$ and using the trapezoidal rule for the right-hand side gives

$$\left(\underline{O} + \mathrm{i}\frac{\delta t}{2}\underline{H}\right)\mathbf{C}(t+\delta t) = \left(\underline{O} - \mathrm{i}\frac{\delta t}{2}\underline{H}\right)\mathbf{C}(t). \tag{4}$$

Thus the propagation of the wavefunction by one step δt reduces to solving a linear equation $\underline{A}\mathbf{x} = \mathbf{b}$, with $\underline{O} + \mathrm{i}\delta t\underline{H}/2$ equalling $\underline{A}$. We directly solved the linear matrix equation using the method described below.

The propagation of Rydberg electrons almost always forces the use of either an implicit propagator or a split operator technique. The reason is that these methods allow time steps related to the physical time of the problem (here the Rydberg period). With a split operator approximation, the Hamiltonian is formally separated into two (or more) pieces, e.g. $H = H_1 + H_2$, and the propagator is approximated as $\exp(-\mathrm{i}H\delta t) \simeq \exp(-\mathrm{i}H_1\delta t/2)\exp(-\mathrm{i}H_2\delta t)\exp(-\mathrm{i}H_1\delta t/2)$. For the basis set representation we use, there does not appear to be an accurate way to split the operators. Thus, we must use the implicit propagator.

There are three properties of the $\underline{A}$ that allow us to go to quite large $\omega_{\max}$. The first is that $\underline{A}$ is symmetric so the linear equation can be solved using a Cholesky decomposition [18] of $\underline{A}$; i.e. $\underline{A}$ can be decomposed into $\underline{L}\underline{L}^T$ where $L_{ij} \neq 0$ only for $i \geqslant j$. This saves a factor of 2 in memory compared to an LU decomposition of $\underline{A}$. The second is that the sparse nature of $\underline{A}$ can be used to reduce the number of elements of $\underline{L}$ that needs to be stored. This is because an enormous fraction of the elements of $\underline{L}$ are 0. The column in which the first nonzero element in a given row of $\underline{L}$ appears is in the corresponding first column where a nonzero element appears in $\underline{A}$. The linear algebra subroutine that takes advantage of this property uses a factor of 9.0 less memory for $\omega_{\max} = 60$ than would be needed for the full $\underline{L}$. This also gives a

large increase in speed since we do not use the 0 elements of $\underline{L}$ in the linear equation solver. The third property is that the propagation is extremely stable and we did not need double precision for $\underline{L}$. This gives another factor of 2 decrease in memory and an increase in speed. These properties allow a factor of 36 decrease in memory requirements and over an order of magnitude increase in speed. As an example, 107 Mb of memory is needed for $\omega_{\max} = 48$ and 204 Mb of memory is needed for $\omega_{\max} = 60$.

In the first situation we modelled in He, we attempted to isolate the analog of the symmetric stretch motion in molecules. Ideas about the symmetric stretch motion in He have evolved tremendously during the past decade. Originally, it was believed that the symmetric stretch motion served as the main mechanism for photo-exciting doubly excited states [19–24]; this seems intuitively obvious since both electrons are originally quite close to the nucleus compared to the size of the doubly excited states. Later it was argued [25, 26] that the symmetric stretch plays almost no role in the photoexcitation of doubly excited states. Two reasons were given for this changed interpretation. The first was that none of the doubly excited eigenstates showed any sort of structure that could be interpreted as arising from symmetric stretch motion. The second was a classical analysis that found an infinite Liaponov exponent arising from the triple collision at $r_1 = r_2 = 0$. The current idea is that doubly excited states are reached by electrons that are launched from $r_1 = r_2 = 0$ at a small but nonzero angle with respect to the $r_1 = r_2, \theta_{12} = \pi$ line. Our calculations tend to confirm this interpretation and eliminate the possibility that a small admixture of 'symmetric stretch motion' is contained in each resonance state.

In our calculations, we estimated the principal quantum number of the Rydberg electrons, n_{Ryd}, using the old quantum theory quantization condition $\oint \mathbf{p} d\mathbf{q} = n\pi$ where n is the number of nodes thus giving $n = 2n_{\mathrm{Ryd}}$. Using this condition gives an outer turning point at $r_f = 2n_{\mathrm{Ryd}}^2/(Z - 1/4)$ and a period of $\tau_{\mathrm{Ryd}} = 2\pi n_{\mathrm{Ryd}}^3/(Z - 1/4)^2$; Z is the charge on the nucleus. For 'symmetric stretch' motion we started the wave packet so that the electron probability was localized to $r_1 \sim r_2 \sim r_f$ and $\theta_{12} \sim \pi$; the momenta in all three directions were localized near 0. By starting the electrons near their outer turning point, we can have 100% of the initial wavefunction where both electrons are approximately on opposite sides of the nucleus at the same distance. The initial state was given by

$$\Psi(q_{12}, q_1, q_2) \propto F_{12}(q_{12}) F(q_1) F(q_2) \tag{5}$$

where the function $F = q^{40} \exp\left(-17.5q/n_{\mathrm{Ryd}}^2\right)$ and the $F_{12} = \exp\left(-50q_{12}^2/n_{\mathrm{Ryd}}^4\right)$. The separability of the wavefunction at $t = 0$ is not important and was only used to facilitate the calculation of the initial coefficients, $\mathbf{C}(0)$.

In figure 1, we plot $|\langle\Psi(0)|\Psi(t)\rangle|$ for several different values of n_{Ryd}. The times have been scaled to be in units of τ_{Ryd}. There are several interesting features to notice in figure 1. The first is the large amount of recurrence to the initial state at times $t \simeq \tau_{\mathrm{Ryd}}$ suggesting that symmetric stretch motion may exist (this interpretation is not quite correct as discussed below). The second feature to notice is that the recurrence is only weakly dependent on n_{Ryd} for times less than ~1.5 periods; this is an effect of the classical scaling of the Hamiltonian which shows that the Heisenberg uncertainty relation is not playing a large role for these short times. However, there is little similarity after this time which shows that quantum effects quickly become important for this type of motion. The third interesting feature is the large fraction (roughly 1/3–1/5) of the wavefunction recurring to the initial packet at long times, $\sim 4\tau_{\mathrm{Ryd}}$, which shows that a large fraction of the packet returns to the region near $r_1 = r_2 = r_f$ and $\theta_{12} = \pi$ and $\mathbf{p}_1 = \mathbf{p}_2 = 0$.

Although the results of figure 1 suggest the possible existence of symmetric stretch motion, a more complicated picture emerges from the time-dependent wave packet. In figures 2 and 3,

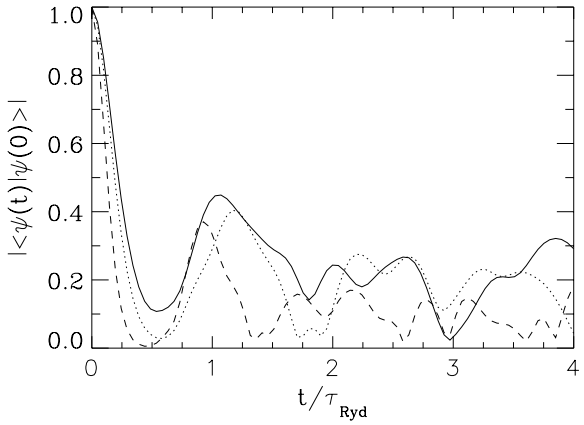

Figure 1. The time-dependent recurrence, $|\langle\Psi(0)|\Psi(t)\rangle|$, for symmetric stretch simulation with $n_{\mathrm{Ryd}} = 10$ (solid line), 13 (dotted line) and 16 (dashed line). The time is scaled by the symmetric stretch period. The initial wavefunctions are scaled with n_{Ryd}; thus, the recurrence should be independent of n_{Ryd} if quantum effects are unimportant.

we plot $\rho = |\psi(r_1, r_2, \theta_{12} = \pi, t)r_1 r_2|^2$ which is the volume weighted electronic density when the electrons are on opposite sides of the nucleus. The results in figure 2 are for $n_{\mathrm{Ryd}} \sim 10$ and in figure 3 are for $n_{\mathrm{Ryd}} \sim 15$. The times are given in increments of $\tau_{\mathrm{Ryd}}/5$ and the radial scales have been chosen to roughly reflect the n_{Ryd}^2 distance scaling. While there is clearly electron probability along the line $r_1 = r_2$, there is also a large fraction of the wave packet that does not travel along this line and reflects off the $r_1 = 0$ line with nonzero r_2 (and off the $r_2 = 0$ line with nonzero r_1). An examination of the sequence of electron probability suggests that there is relatively little motion along the $r_1 = r_2$ line although the initial state is originally localized to this line with zero velocity. The wave packet falls off of the unstable line so quickly that the region near $r_1 = r_2 = 0$ does not play a major role in the dynamics. An interesting consequence of the electron distribution rapidly deviating from the $r_1 = r_2$ line is that the two electrons cannot easily exchange energy with each other. The electrons need to get somewhat close to each other in order to efficiently exchange energy and angular momentum. This partly explains why there is a large recurrence to the initial position.

The wavefunction at times $2\tau_{\mathrm{Ryd}}/5$ and $3\tau_{\mathrm{Ryd}}/5$ varies much faster in space than at the other times because an electron's velocity is much higher when it is near the nucleus; the fast variation arises from the interference of the inward and outward moving electron wave near the nucleus. The interference pattern at $t = 2\tau_{\mathrm{Ryd}}/5$ is consistent with a standing wave pattern resulting from electrons reflecting from $r_1 = 0$ (and large r_2) and vice versa. The wavelength near the nucleus (small r_1 or r_2) is roughly the same in figures 1 and 2 but appears smaller in figure 2 because of the change in scale. The interference patterns are a very sensitive measure of the underlying dynamics and can show substantial changes from non-dominant interactions. A very interesting change can be noticed between $2\tau_{\mathrm{Ryd}}/5$ and $3\tau_{\mathrm{Ryd}}/5$. At $2\tau_{\mathrm{Ryd}}/5$, the minima and maxima of the quickly varying part of the wavefunction fairly closely follow $r_1 =$ constant or $r_2 =$ constant lines but for times larger than or equal to $3\tau_{\mathrm{Ryd}}/5$ the minima and maxima only approximately follow $r_1 =$ constant or $r_2 =$ constant lines. If we artificially set the inter-electron repulsion to 0 but use the same initial state as in the full calculation, then the minima and maxima follow $r_1 =$ constant or $r_2 =$ constant lines for all times. This shows that the $1/r_{12}$ interaction does not cause effective correlation until times later than $2\tau_{\mathrm{Ryd}}/5$. Although not the cause of the dominant effects, the $1/r_{12}$ interaction

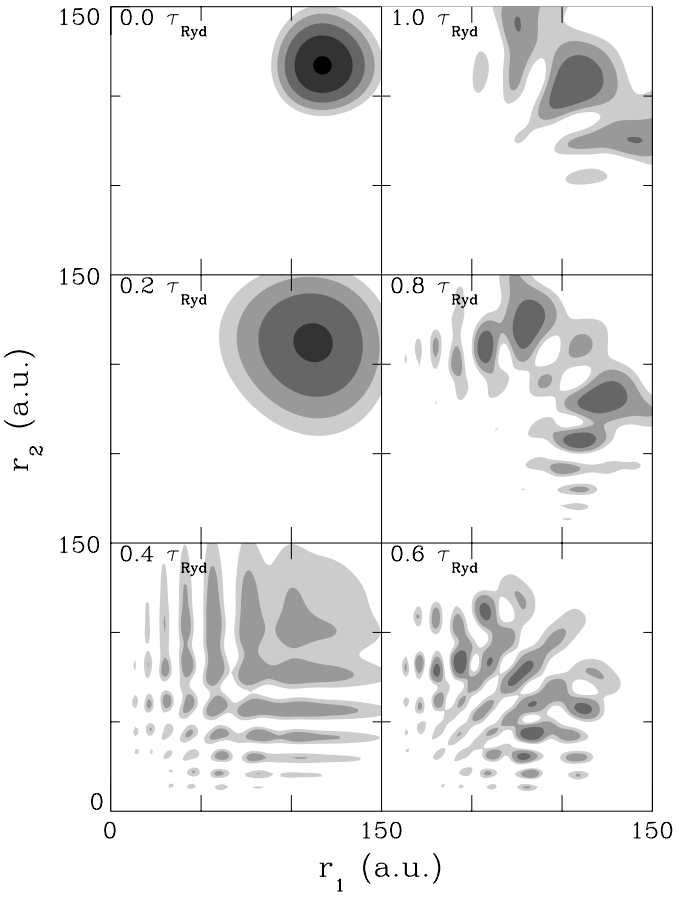

Figure 2. The volume weighted electron density for $\theta_{12} = \pi$ for $n_{\rm Ryd} \simeq 10$ simulation of symmetric stretch motion. The times are in increments of $\tau_{\rm Ryd}/5$. The contours are the same in all figures and the decrease in probability between successive contours is a factor of 2.

does change the wavefunction. For example, notice that there is a hole in the distribution in figure 3 near the starting value of $r_1 = r_2$ at $t = \tau_{\rm Ryd}$.

We performed classical calculations where we gave the electrons the same spatial distribution in the $\theta_{12} = \pi$ plane as the quantum distribution but set their initial momentum equal to zero and started all electrons in the $\theta_{12} = \pi$ plane. The asterisk in each of the frames of figure 3 marks the positions of classical electrons that start at the peak of the wavefunction at $t = 0$ with zero velocity. For all trajectories, the electrons are initially stationary and the starting position is marked by a + and the final position is marked by a $\times$. The final time is the same as for the figure where the trajectory is plotted.

At $t = 0$, the maximum of the quantum distribution in figure 3 is at the point (257, 257) au. From a comparison with classical calculations, we found that some of the features in the wavefunction at the later times, $4\tau_{\rm Ryd}/5$ and $\tau_{\rm Ryd}$, appear to have a correspondence with the classical distribution at these times. Three classical trajectories are given in figure 3. It is interesting to note that the closer the starting point is to $r_1 = r_2$ the more energy is exchanged between the electrons and the further the final point is from $r_1 = r_2$; if the initial point is at $(257 + \Delta, 257 - \Delta)$, then all $\Delta < 15$ give final points outside of the graphed region except

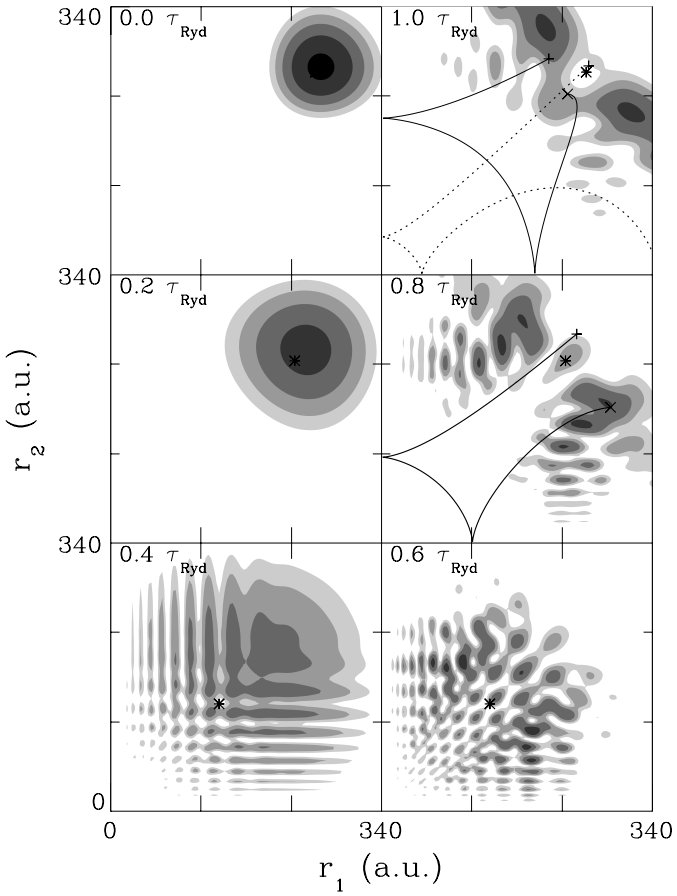

Figure 3. Same as figure 2 but for an $n_{\mathrm{Ryd}} \simeq 15$ simulation. The position of classical electrons that start at the peak of the wavefunction at $t = 0$ is marked with an asterisk in each frame. The classical trajectories start with zero velocity at the + at $t = 0$ and end at the $\times$ at the time of the panel. The trajectory in the $0.8\tau_{\mathrm{Ryd}}$ frame starts at (245, 265) and ends at (296, 172). The solid line trajectory in the $1.0\tau_{\mathrm{Ryd}}$ frame starts at (210, 274) and ends at (228, 229) while the dotted line trajectory starts at (260, 265) and ends at (522, 87). The trajectory that starts closest to the point $r_1 = r_2$ approaches most closely to $r_1 = r_2 = 0$ and has the largest energy exchange between the electrons.

$\Delta = 0$. The largest probability for $4\tau_{\mathrm{Ryd}}/5$ is at roughly (300, 175) and (175, 300) au and for τ_{Ryd} is at roughly (320, 170) and (170, 320) au. The classical distribution also shows a large probability in these regions. This feature apparently arises from trajectories similar to those in the $4\tau_{\mathrm{Ryd}}/5$ frame which starts in a region of high probability at $t = 0$ but is far enough from the $r_1 = r_2$ to prevent large exchange of energy. Some features are not apparent in the classical distribution; for example, the large accumulation of probability at the $r_1 = r_2$ line at τ_{Ryd} is absent in the classical calculation. However, there are classical trajectories that start with a non-negligible probability and reach this region at τ_{Ryd}; an example trajectory is given in the τ_{Ryd} frame. Trajectories that start with $\theta_{12} \neq \pi$ or constructive interference between trajectories that start on opposite sides of the $r_1 = r_2$ line but end on $r_1 = r_2$ are two possible explanations for the large probability at $r_1 = r_2$.

We performed quantum calculations where we kept the initial wavefunction the same but changed the inter-electron repulsion term from $1/r_{12}$ to Z_{12}/r_{12} and observed several trends as we varied Z_{12} from 0 to 1. The same effect can be obtained by increasing the nuclear charge and scaling the lengths and times. At $t = \tau_{\rm Ryd}$, the norm of the wavefunction was less than 1 by an amount[3] that increased monotonically with Z_{12}; over the range $0 \leqslant Z_{12} \leqslant 1$, the decay rate as a function of Z_{12} increased faster than Z_{12} but not as fast as Z_{12}^2. The recurrence to the initial state as measured by $|\langle\Psi(0)|\Psi(t)\rangle|$ peaked for $t > 0$ at $t \simeq \tau_{\rm Ryd}$. The height of the first recurrence peak decreased with increased repulsion because the electrons could more efficiently exchange energy and angular momentum and thus reach different regions of space. Also, the time where this peak occurred increased with increased repulsion because the classical time to return to the region $r_1 \sim r_2$ increases with Z_{12} for 'symmetric stretch' motion.

The results presented here demonstrate that an understanding of the time evolution of two highly excited electrons is possible and may in the future provide an improved picture of the boundary between quantum and classical physics. These calculations for He are simply the first of a series of investigations that can be now performed. It would be interesting to explore the behaviour of other simple motions as $n_{\rm Ryd}$ increases. For example, the bend vibration and the asymmetric stretch motion are obvious motions that can be investigated; because the classical motion simply scales with energy, an investigation with increasing $n_{\rm Ryd}$ would be interesting because one can simulate the same motion but in regions where quantum effects are less or more important. It would also be interesting to investigate the applicability of semiclassical methods to He wave packets since previous semiclassical studies have focused on the time-independent features of this system; it is unclear how long a semiclassical propagation would reproduce the main features of a quantum calculation. It would be interesting to compare and contrast the time dependence of wave packets when starting in a region of phase space that is classically chaotic versus a region that is regular. It would be interesting to know how the one electron density matrix evolves with time for different levels of excitation. Finally, it is easy to change the charge of the nucleus (for example, make wave packets in H^-) or of one of the light particles (for example, make wave packets on $p + e^- + e^+$) and investigate the behaviour of wave packets for several distinct systems. The propagation of double Rydberg wave packets opens a broad region of theoretical research which will increase our knowledge of how energy and probability move amongst several coupled motions.

Acknowledgment

FR is supported by the NSF and RCF is supported by NSF grant no PHY-0244066.

References

[1] Henle W A, Ritsch H and Zoller P 1987 *Phys. Rev.* A **36** 683
[2] Alber G and Zoller P 1991 *Phys. Rep.* **199** 231
[3] Wang X and Cooke W E 1991 *Phys. Rev. Lett.* **67** 1496
Wang X and Cooke W E 1992 *Phys. Rev.* A **46** 4347
[4] Story J G, Duncan D I and Gallagher T F 1993 *Phys. Rev. Lett.* **71** 3431
[5] Schumacher D W, Duncan D I, Jones R R and Gallagher T F 1996 *J. Phys. B: At. Mol. Opt. Phys.* **29** L397
[6] Schumacher D W, Lyons B J and Gallagher T F 1997 *Phys. Rev. Lett.* **78** 4359

[3] The norm of the wavefunction decreases because we used a mask function to prevent reflection from the edge of the basis. This decrease means that probability has moved out of the region covered by our basis set. At $t = \tau_{\rm Ryd}$, the norm decreased to roughly 0.88. The 12% decrease is within a factor of 2 of what we estimated from a classical calculation and is consistent with autoionizing rates from states of lower $n_{\rm Ryd}$.

[7] Robicheaux F and Hill W T III 1996 *Phys. Rev.* A **54** 3276
[8] Pisharody S N and Jones R R 2004 *Science* **303** 813
[9] Lankhuijzen G M and Noordam L D 1996 *Phys. Rev. Lett.* **76** 1784
[10] Robicheaux F and Shaw J 1996 *Phys. Rev. Lett.* **77** 4154
Robicheaux F and Shaw J 1997 *Phys. Rev.* A **56** 278
[11] Jones R R and Noordam L D 1997 *Adv. At. Mol. Phys.* **38** 1
[12] Naudeau M L, Sukenik C I and Bucksbaum P H 1997 *Phys. Rev.* A **56** 636
[13] Fassbinder P, Schweizer W and Uzer T 1997 *Phys. Rev.* A **56** 3626
[14] Bensky T J, Campbell M B and Jones R R 1998 *Phys. Rev. Lett.* **81** 3112
[15] Richter K and Wintgen D 1993 *J. Phys. B: At. Mol. Opt. Phys.* **26** 3719
[16] Rost J M *et al* 1991 *J. Phys. B: At. Mol. Opt. Phys.* **24** 2455
[17] Bürgers A, Wintgen D and Rost J M 1995 *J. Phys. B: At. Mol. Opt. Phys.* **28** 3163
[18] Press W H, Teukolsky S A, Vetterling W T and Flannery B P 1992 *Numerical Recipes* 2nd edn (Cambridge: Cambridge University Press)
[19] Fano U 1983 *Phys. Rep.* **46** 97
[20] Rau A R P 1983 *J. Phys. B: At. Mol. Phys.* **16** L699
[21] Watanabe S and Lin C D 1986 *Phys. Rev.* A **34** 823
[22] Rost J M and Briggs J S 1989 *J. Phys. B: At. Mol. Opt. Phys.* **22** 3587
[23] Sadeghpour H R and Greene C H 1990 *Phys. Rev. Lett.* **65** 313
[24] Harris P G *et al* 1990 *Phys. Rev.* A **42** 6443
[25] Richter K and Wintgen D 1990 *J. Phys. B: At. Mol. Opt. Phys.* **23** L197
[26] Ezra G S, Richter K, Tanner G and Wintgen D 1991 *J. Phys. B: At. Mol. Opt. Phys.* **24** L413